Electrochemical Conversion of NO to NH$_3$ in a PEM Cell

Bunea, Sorin; Coppens, Manoj; Urakawa, Atsushi

Citation (APA)
Bunea, S., Coppens, M., & Urakawa, A. (2023). Electrochemical Conversion of NO to NH$_3$ in a PEM Cell. *ACS Catalysis*, *13*(17), 11345-11351. https://doi.org/10.1021/acscatal.3c01600

Important note
To cite this publication, please use the final published version (if applicable).
Please check the document version above.

Research Article

Electrochemical Conversion of NO to NH₃ in a PEM Cell

Sorin Bunea, Manoj Coppens, and Atsushi Urakawa*

Cite This: *ACS Catal.* 2023, 13, 11345−11351

Read Online

ACCESS | 📊 Metrics & More | 📄 Article Recommendations | 🆘 Supporting Information

ABSTRACT: The continuous electrochemical NO reduction to ammonia in a PEM cell was investigated in this work. We used a ruthenium-based catalyst at the cathode and an iridium oxide catalyst at the anode. The highest ammonia faradaic efficiency was observed at 1.9 V cell voltage. Adjusting the NO flow allowed to achieve 97% NO conversion and 93% ammonia faradaic efficiency for a 5.2% NO/He feed. The ammonia yield was 0.51 mmol cm^{-2} h^{-1}, among the highest reported to date with the advantage of continuous operation. Experiments with a low NO concentration feed of 983 ppm showed 98% conversion at 0 V vs pseudo-RHE. Achieving this performance under such mild conditions indicates the great potential of the PEM cells for NO_x abatement applications and the production of valuable NH₃.

KEYWORDS: *polymer electrolyte membrane, NO reduction, electrochemical ammonia synthesis, electrocatalysis, ruthenium catalyst*
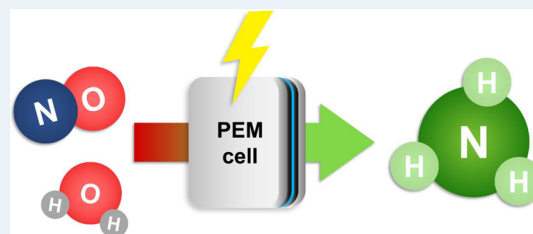
■ INTRODUCTION

The anthropogenic perturbation of the natural nitrogen cycle represents a concerning threat to the environment. NO_x gases emitted by fossil fuel power plants and automobile engines contribute to the formation of acid rain and smog and are harmful to the natural environment and human health.[1] The development of the selective catalytic reduction (SCR) technology and the implementation of such units in power plants have significantly decreased NO_x emissions over the last decades.[2] However, the operational costs of SCR are high due to the requirement of continuous ammonia or urea supply, and the resulting dinitrogen gas does not represent a valuable product from a commercial point of view. It would be more desirable to convert NO_x gases to a useful chemical such as ammonia. The market price for ammonia is around 500$ per ton. Currently, ammonia is produced via the energy-intensive Haber−Bosch process, which is responsible for 1% of the yearly global CO_2 emissions.[3] The electrochemical NO_x reduction to ammonia could represent a possible solution for decentralized on-demand small-scale ammonia production, powered by renewable electricity. Thermal power plants emit an average of 1 kg NO_x per MWh.[4] For a typical 500 MW size plant, this translates into ca. 3000 tons of NO_x per year.

As the global population is expected to increase over the following decades, so will the production of nitrogen-based fertilizers to meet the growing demand for food.[5] At the same time, the effects of anthropogenic activity over the last 200 years become increasingly noticeable, impacting the environment in a catastrophic manner. The Paris Agreement, adopted in 2016, aims to curb CO_2 emissions to keep Earth's temperature increase under 1.5 °C compared to preindustrial levels. In this context, it is clear that alternative processes for

ammonia production need to be developed to aid the achievement of this ambitious goal.

The electrochemical nitrogen reduction reaction (NRR) to ammonia has gained significant research interest over the last decade.[6−9] Nevertheless, reported faradaic efficiency (FE) and nitrogen conversion are far from commercially relevant values. The main reason for low efficiency is the high chemical stability of the nitrogen molecule. Efforts of electrochemically activating nitrogen have proved inefficient to date.

An alternative path is to convert the harmful reactive nitrogen species, such as NO_x, to ammonia by using renewable electricity, closing the reactive nitrogen cycle (Figure 1).

The technological process of nitrogen fixation via nitric oxide is more than a century old, based on the reaction of nitrogen oxidation first documented by Cavendish.[10] It has been actually implemented on a large scale as the Birkeland−Eyde process at the beginning of the twentieth century. The process used electric arc discharge for reacting nitrogen with oxygen to produce nitric oxide, which was subsequently converted to nitrates for use in agriculture. Unfortunately, due to very large energy requirements and the advent of the economic Haber−Bosch process using fossil fuels, the Birkeland−Eyde process was quickly replaced by the new process.[11] Nevertheless, in the context of the depletion of fossil fuels and the impact of huge carbon emissions associated with the Haber−Bosch process, the interest in alternative nitrogen
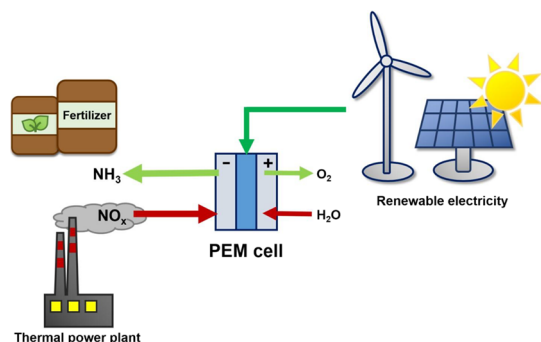
Figure 1. Concept of the continuous electrochemical ammonia synthesis process from NO_x and renewable electricity in a polymer electrolyte membrane (PEM) cell.

activation routes involving NO has increased in recent years.[12−16] Nitrogen oxidation to NO would represent the first step in a two-step process of sustainable ammonia synthesis. The second step would represent the NO reduction reaction to ammonia, which is the main topic of this work.

The electrochemical NO reduction reaction (NORR) targeting hydroxylamine production was investigated in the 1970s.[17−19] In those studies, ammonia was regarded as a by-product and considered undesirable. In recent years, more studies emphasizing ammonia formation emerged.[20−24] Faradaic efficiencies to ammonia as high as 100% were achieved.[23] Nevertheless, most studies report the use of metallic electrodes immersed in liquid electrolytes in batch systems. For large-scale industrial applications, a gas flow reactor would be more desirable due to the advantages of continuous operation, thus avoiding the need for an ammonia stripping unit to separate it from the liquid cathode feed.

In this work, a polymer electrolyte membrane (PEM) electrolysis cell using a Ru/C cathode catalyst was employed for the gas phase NORR. The cathodic NORR was combined with water oxidation or hydrogen oxidation at the anode of the cell, to prove the versatility of the operation. When the hydrogen oxidation reaction (HOR) takes place at the anode, an OCP of ca. 0.85 V was recorded, and at low current densities, the cell can be concomitantly used for electricity generation. A schematic representation of the two approaches is presented in Figure 2.

RESULTS AND DISCUSSION

Experiments with Water Oxidation at the Anode. The choice of Ru/C catalyst was based on our previous experience with this catalyst in electrochemical nitrate reduction studies in a PEM cell.[25] There, it exhibited high FE and selectivity toward
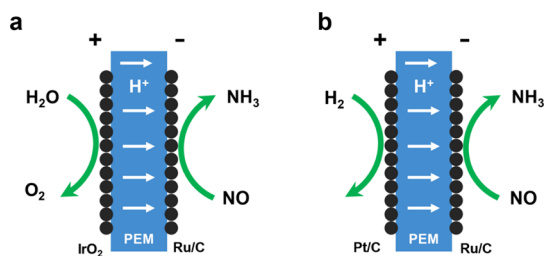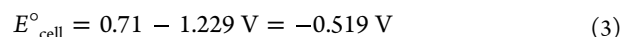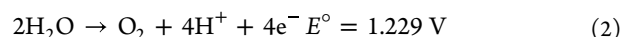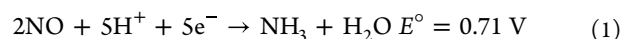

Figure 2. Schematic representation of NO reduction at the cathode of a PEM cell with (a) water oxidation and (b) hydrogen oxidation at the anode.

ammonium. As NO is an intermediate species in the electrochemical nitrate reduction mechanism, we expected to observe a similar trend in the activity of the ruthenium catalyst. The X-ray diffraction pattern, as well as the microscopic structure of the catalyst, is presented in Figures S2 and S3.

We investigated a cell voltage range between 1.7 and 2.1 V. Constant voltage experiments were carried out for 30 min. Considering the standard reduction potentials in eqs 1 and 2, the thermodynamic potential of a cell with nitric oxide reduction taking place at the cathode and water oxidation at the anode is $E^{\circ}_{cell} = -0.519$ V (eq 3). Nevertheless, due to competing hydrogen evolution reaction (HER), and difficulties in implementing a reference electrode in a PEM cell, the cell voltage range investigated during experiments was significantly higher.

$$2NO + 5H^+ + 5e^- \rightarrow NH_3 + H_2O \; E^{\circ} = 0.71 \text{ V} \quad (1)$$

$$2H_2O \rightarrow O_2 + 4H^+ + 4e^- \; E^{\circ} = 1.229 \text{ V} \quad (2)$$

$$E^{\circ}_{cell} = 0.71 - 1.229 \text{ V} = -0.519 \text{ V} \quad (3)$$

The FE toward different NO reduction products as a function of cell voltage, together with the average current density recorded during the experiments, is presented in Figure 3.

The ammonia FE exhibited a promising value of ca. 50% already at the lowest cell voltage tested (1.7 V) with a current density of 32 mA cm^{-2}. The FE increased with cell voltage, exhibiting a maximum of ca. 78%, at 1.9 V, at a current density of ca. 64 mA cm^{-2}. At 2−2.1 V, the FE of ammonia decreased, and an increase in hydrogen FE was observed. The cause for the increase in hydrogen FE is the high recorded current densities at 2 and 2.1 V, leading to an imbalance in the reaction rates at the anode (water oxidation) and the cathode (NO reduction). Under these conditions, a higher amount of protons were generated at the anode, resulting in a higher recombination rate to produce molecular hydrogen at the cathode of the cell, similar to our observations in electrochemical nitrate reduction experiments.[25] The NO conversion values are similar compared to the changes in the NH$_3$ current density and NH$_3$ FE (Figure 4). The most important point of this figure together with the information contained in Figure 3 is about how the electrons are used and which reaction pathways are accelerated over others. At a low cell potential (e.g., 1.7 V), the NO conversion is high but selectivity to NH$_3$ is poor because of the dominant formation of N$_2$O and N$_2$ (Figure 3b). This clearly indicates that NO activation is very good even at this low cell potential, but the potential is not sufficiently reductive to achieve selective NH$_3$ formation. On the other hand, at the high cell potential (e.g., 2.1 V), NO conversion is similar and selectivity to NH$_3$ is very good (Figure 3b). However, this does not tell the whole story since the selectivity shown in Figure 3b is based on nitrogen-containing compounds. At this high cell potential, HER becomes significant (Figure 3a) and this is where electrons end up. Figure 4 shows that the amount of protons generated at the anode is affected by the loading of IrO$_2$ and too much IrO$_2$ at the anode drives HER favorably (Figure 4c at 2.1 V—the large drop of NH$_3$ FE with 2 mg cm^{-2} IrO$_2$ due to dominant HER). Hence, an optimum condition lies in between where the cathodic potential is negative to drive NH$_3$ formation, while HER does not become dominant by forming too much proton
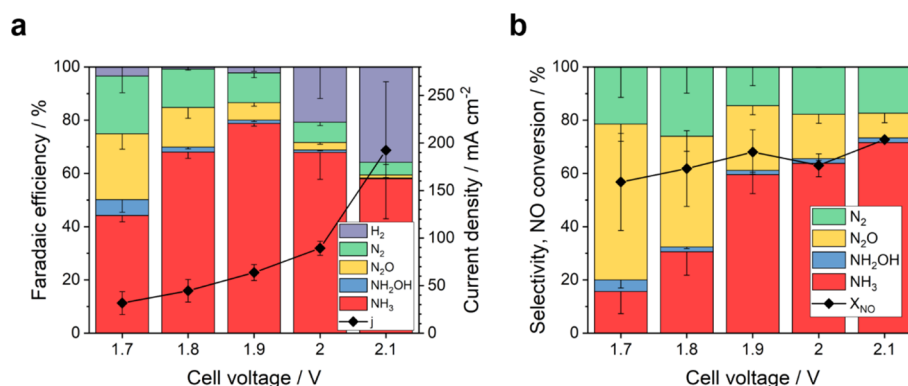
Figure 3. (a) FE toward various products in the NO reduction and current densities at varying cell voltage and (b) NO conversion and selectivity to various nitrogen products as a function of cell voltage.
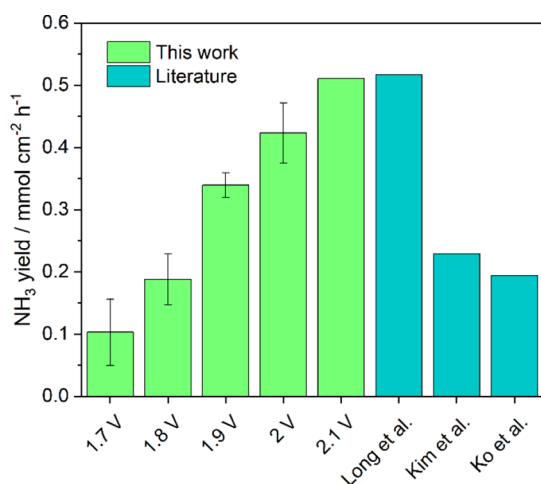

Figure 4. Comparison between NORR ammonia yield rates in our work and the literature.[21,23,24]

at the anode or performing the reaction at too high a cell potential.

Nitrogen formation was observed at cell voltages as low as 1.7 V. Despite the lowered FE to N_2 at higher cell voltage, N_2 selectivity among the N-containing products remained relatively constant over the whole investigated cell voltage range (Figure 3b). As reported in our previous studies, it is possible that nitrogen formation does not follow an electrochemical transformation pathway, but rather follows an electrolysis-assisted hydrogenation route.[26] In this latter pathway, the hydrogen is evolved in situ at the cathode and

reacts with nitric oxide at the catalyst surface. This pathway is not strongly affected by the electrode potential, leading to the relatively constant N_2 selectivity over the investigated cell voltage range.

N_2O formation appeared more favorable at low cell voltage, showing a considerable FE of 28% at 1.7 V, which decreased to 2% at 2.1 V. This is in good agreement with the literature, which reports N_2O formation dominating at high potentials (0.3−0.7 V vs RHE).[27] In our case, this represents the low cell voltage region. In the literature, more favored ammonia formation has been reported at low potentials (<0.3 V vs RHE).[28] In our case, this condition is reflected in the high cell voltage region. Hydroxylamine formation was also detected, although the amounts were low throughout the investigated cell voltage range. The highest recorded FE for hydroxylamine was 6.5% at 1.7 V cell voltage. At higher cell voltages, it dropped below 2%.

The ammonia FE as a function of cell voltage greatly resembles the trends observed in our work on aqueous nitrate reduction with the same ruthenium catalyst.[25] This suggests that the reaction proceeds via a similar mechanism. In nitrate reduction, adsorbed NO may be an important reaction intermediate, from which various products can emerge.[29] Furthermore, as it is likely that the catalyst−ionomer interface is wet during operation due to water diffusion from the anode side, NO may be absorbed in the wet ionomer phase and subsequently undergo transformation to ammonia.

Overall, the obtained ammonia yield (0.51 mmol cm^{-2} h^{-1} at 2.1 V cell voltage with an FE of 57%) was among the highest reported in the literature (Figure 4). Furthermore, the reaction
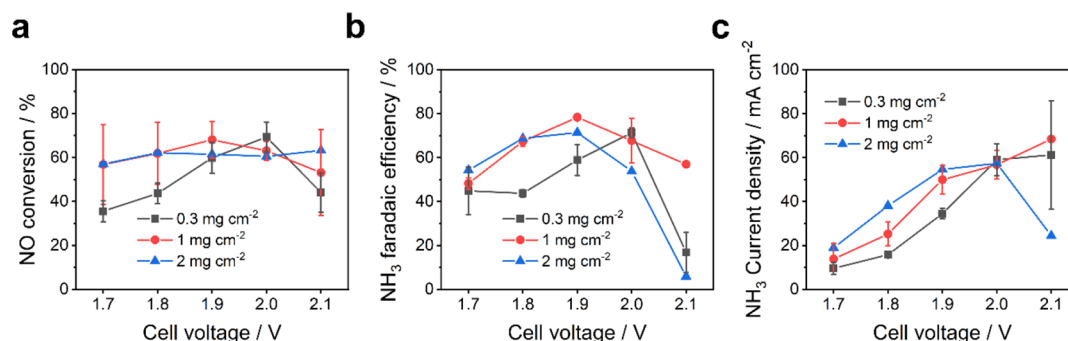

Figure 5. (a) NO conversion, (b) ammonia partial current density, and (c) FE as a function of cell voltage for MEAs with different iridium oxide anode catalyst loadings.

was implemented in a flow reactor which is more practical for scale-up, compared to the generally reported cells with liquid electrolytes.[21,23,24] Our study demonstrates that NORR in a PEM cell is able to surpass the performance obtained in most reports using batch cells, making the approach attractive for scaling up.

Impact of Anode Catalyst Loading. The above results show promising activity in NORR toward ammonia. At the same time, the competitive and dominating HER leads to low ammonia FE at cell voltages above 2 V. To investigate the importance of the balance between the anode and cathode reaction rates, experiments with different iridium oxide loadings at the anode were conducted.[25] The rates of water oxidation and proton generation are dependent on the number of active sites on the catalyst surface at the anode. If the anode catalyst loading is too high, elevated current densities can be achieved in the PEM cell, but most of the electrons are inefficiently used in the undesired reaction of proton recombination to produce hydrogen at the cathode, unless a hindrance for HER is in place. In the experiments described in this section, the cathode catalyst loading over membrane electrode assemblies (MEAs) was kept constant at 2.5 mg cm^{-2}, while iridium oxide loadings were varied: 0.3, 1, or 2 mg cm^{-2}.

Figure 5a shows that at cell voltages between 1.7 and 1.9 V, NO conversion increases with iridium oxide loading from 0.3 to 1 mg cm^{-2}. No significant difference can be observed between MEAs with 1 and 2 mg cm^{-2} iridium oxide loading. At 2.0 V, a similar performance for the three MEAs was recorded. At 2.1 V, the 1 mg cm^{-2} IrO_2 MEA was found as the best performing. The ammonia partial current density (Figure 5b), which is obtained by multiplying FE and total current density, indicates that for 0.3 mg cm^{-2} IrO_2 MEA, the proton generation rate at the anode is low, causing the poorer NO conversion observed in Figure 5a. For the 1 and 2 mg cm^{-2} IrO_2 MEAs, ammonia partial current density increases with iridium oxide loading, in the 1.7−2.0 V cell voltage range, indicating increased ammonia production at higher cell voltages. At 2.1 V, the 1 mg cm^{-2} MEA exhibited even higher ammonia partial current density, reaching ca. 70 mA cm^{-2}. The performance of the 2 mg cm^{-2} MEA was poorer at this elevated voltage: the ammonia partial current density dropped to ca. 30 mA cm^{-2}. This is associated with an increased FE for hydrogen (Figure S5). At the same time, the ammonia FE decreases with the increase of iridium oxide loading from 1 to 2 mg cm^{-2} (Figure 5c) at cell voltages above 1.8 V, despite the increasing ammonia partial current density and production. The likely explanation for this observation is that NORR to ammonia proceeds via a heterogeneous electrolysis-assisted hydrogenation mechanism (i.e., NO reduction by produced H_2) at cell voltages above 1.9 V. This mechanism has been reported in the literature for the electrochemical reduction of nitrate to nitrogen.[26,30] This hypothesis is supported by the observation of a higher ammonia production yield for the MEA with 2 mg cm^{-2} iridium oxide loading (Figure S4). It is also notable that the highest ammonia yield was observed at 2.1 V cell voltage for the 1 mg cm^{-2} MEA, where ammonia FE exhibited a modest value of 57%, but NO conversion was highest (ca. 70%) along with the ammonia partial current density (ca. 70 mA cm^{-2}). The iridium oxide loading variation allowed us to identify the optimum loading for achieving the highest ammonia FE. In conclusion, 2 mg cm^{-2} is the typical loading for PEM water electrolyzers, but due to the high costs

of iridium oxide, it is generally desirable to use lower loadings.[31] For further experiments in this study, the intermediate iridium oxide loading of 1 mg cm^{-2} was used to test the lower loading and advantageous FE to NH_3. Loading as low as 0.3 mg cm^{-2} IrO_2 over membranes is technically challenging due to inhomogeneities that arise during catalyst spray coating deposition, as well as catalyst loss during catalyst ink handling and transfer.

Toward Complete Single-Pass NO Conversion. After identifying FE and conversion trends as a function of cell voltage, our next goal was to maximize NO conversion by optimizing reaction conditions further. One of the parameters that are easy to tune is the gas flow through the cathode compartment of the PEM cell. It is expected that higher NO conversion can be achieved at a low flow rate due to a longer residence time of NO molecules in the PEM cell. The flow variation experiments were conducted at 1.9 V cell voltage, where the best performance was observed in terms of ammonia FE and NO conversion. At 8 mL min^{-1} 5.2% NO/He flow, 97% single-pass conversion was achieved in the PEM cell (Figure 6). However, the FE toward ammonia is lower under
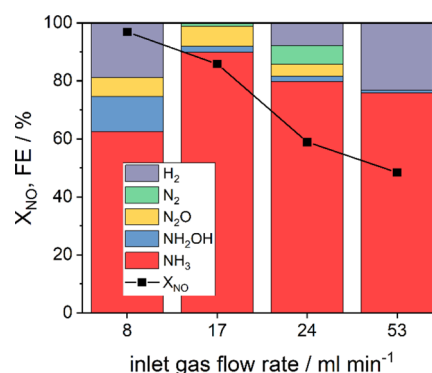

Figure 6. NO conversion (X_{NO}) and FE toward ammonia as a function of inlet gas flow rate at 1.9 V cell voltage, 1 mg cm^{-2} IrO_2 MEA.

these conditions, likely due to the low reactant availability at the catalyst surface at high conversion and proton recombination to hydrogen.

At an increased flow rate, NO conversion decreased. The lowest value of 48% was recorded at 53 mL min^{-1} gas flow. The decrease in conversion with the increasing flow rate of the inlet stream can be explained by the lower contact time between the reactant and the catalyst. An even higher ammonia FE was found at the lower flow rate of 17 mL min^{-1} than at 24 mL min^{-1} of the previous experiments (Figure 3). NH_3 FE showed a further decrease at 53 mL min^{-1} flow, reaching 80%. This was accompanied by an increase in current density and an increase in hydrogen evolution (Table S2). This could be due to less efficient contact of NO with the catalyst or less efficient NO absorption in the ionomer. Another possibility is the drying of the catalyst/ionomer interface at high gas flows.

Experiments with Hydrogen Oxidation at the Anode. We further explored the possibility of operation with hydrogen oxidation at the anode. This may allow for more precise control of the competing HER, yielding higher FE toward ammonium, besides studying cathodic potential more independently.[25]
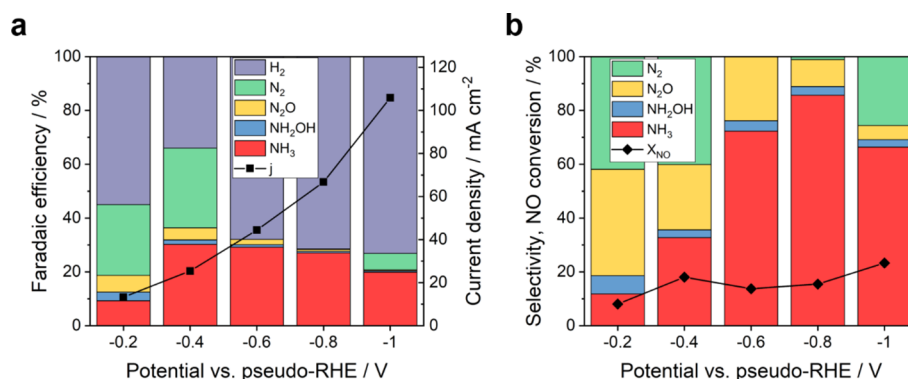
Figure 7. (a) FE with recorded current density and (b) NO conversion and selectivity to nitrogen reduction products as a function of applied potential (vs pseudo-RHE). 2.5 mg cm^{-2} 40 wt % Ru/C cathode catalyst, 1.5 mg cm^{-2} 40 wt % Pt/C anode catalyst, 50 mL min^{-1} H$_2$ anode feed.

A similar approach has been reported and referred to as "electrogenerative nitric oxide reduction", suggesting a galvanic cell (fuel cell) operation mode.[18,19] Porous platinum and ruthenium black were used as cathode catalysts in various acidic electrolytes, like HClO$_4$, HCl, H$_2$SO$_4$, H$_3$PO$_4$, and HNO$_3$. Almost full NO conversion was achieved for the Pt electrode. The selectivity was strongly influenced by the choice of electrolyte. For Ru, a higher ammonia selectivity was observed, although, similar to Pt, it varied strongly with the used electrolyte.

Considering the standard reduction potential of nitric oxide to ammonia (eq 4), coupled with HOR at the anode (eq 5), a theoretical cell potential of 0.836 V is obtained (eq 6).

$$2NO + 5H^+ + 5e^- \rightarrow NH_3 + H_2O \quad E° = 0.71 \text{ V} \quad (4)$$

$$H_2 \rightarrow 2H^+ + 2e^- \quad E° = 0 \text{ V} \quad (5)$$
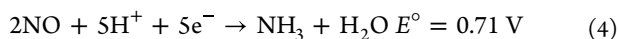
$$E°_{cell} = 0.71 - 0 \text{ V} = 0.71 \text{ V} \quad (6)$$

In our work, an open circuit potential of ca. 0.6 V was measured. However, reduction products could not be detected in the voltage range reported by Langer and Page, 0−0.6 V, and very low current densities were recorded during our experiments.[18,19] Since our main goal was to achieve as high NO conversion to NH$_3$ as possible, potentials more negative than 0 V were applied to drive the transformation (Figure 7a). For the anode compartment of the cell, where a platinum catalyst and a hydrogen feed were used, the assumption of pseudo-RHE reference electrode holds at low current densities. Therefore, for these experiments, the applied potentials are reported vs pseudo-RHE.

The most striking observation is the considerably higher FE toward hydrogen at comparable current densities to experiments with water oxidation at the anode. An explanation for the higher concentration of hydrogen in the outlet stream could be its crossover from the anode to the cathode compartment through the Nafion membrane, altering the FE values of nitrogen-containing species. However, we estimated the hydrogen crossover rate using the method described by Cheng et al.[32] According to this method, for our experiments, hydrogen crossover would only account for a maximum of 6% increase in FE for the hydrogen product detected at the cathode. This significant difference in FE was not observed in our liquid-phase nitrate reduction experiments. The experiments with hydrogen oxidation at the anode involved gas phase operation of the cell both at the anode and cathode, in contrast to experiments with water oxidation at the anode,

where the MEA was fully hydrated on one side. It is likely that MEA or ionomer layer hydration plays a role in achieving high FE toward ammonia.

The lowest FE toward ammonia (ca. 9%) was observed at the lowest applied potential of −0.2 V vs pseudo-RHE. It reached a maximum FE of 30% at −0.4 V vs pseudo-RHE. At more negative cell voltages, a slight decrease was observed with the ammonia FE of 20% at −1 V vs pseudo-RHE, accompanied by an increase in hydrogen formation.

The NO conversion was also significantly lower compared to experiments with water oxidation at the anode (Figure 7b vs Figure 3b). It increased upon shifting applied potentials to more negative values, reaching a maximum of ca. 30% at −1 V vs pseudo-RHE. Interestingly, ammonia selectivity showed a maximum at −0.8 V vs pseudo-RHE (ca. 85%), which is different from the potential at which the highest FE was observed (−0.4 V vs pseudo-RHE). This is different from the previous observations both for NORR experiments with water oxidation at the anode and nitrate reduction experiments, where the highest ammonia FE and selectivity were generally observed at the same cell voltage. This difference could be caused by hydrogen crossover through the membrane. Subsequently, higher H$_2$ concentrations might become available at the catalyst surface, leading to a higher NO hydrogenation rate, and higher selectivity to ammonia as a result.

Overall, the performance of NORR to ammonia with hydrogen oxidation at the anode was not as high as in the experiments with water oxidation at the anode. Generally, we found the cell operation with gases both at the cathode and anode more challenging. In the first experiments that we conducted, we found that gas humidification and electrode flooding play an important role in the long-term stability of the cell. This issue has also been extensively explored and tackled in fuel cell research.[33] The optimization of these aspects was not conducted in this study, but it should allow for achieving comparable performance to experiments with water oxidation at the anode.

NORR as Potential NO$_x$ Abatement Technology. Experiments described in the previous sections were conducted with a 4.8% NO/He mixture. In practice, such high NO concentrations might not be accessible in typical NO sources, such as power plants and car exhaust streams. NO$_x$ concentration in such feeds is typically between 500 and 1000 ppm.[34] To investigate the applicability of NORR in PEM cells for more realistic NO$_x$-containing feeds, we conducted

experiments with a 983 ppm NO/He mixture. In this case, the formed ammonia was not collected in the acid trap, and a condenser was used to remove the majority of water and ammonia after the PEM cell, which interfered with our established transmission-IR quantification method at such low NO concentration (Figure S1). Therefore, we only investigated whether a relevant single-pass NO conversion can be achieved for low NO concentration streams.

As shown in Figure 8, NO conversion reaches 40% already at 0 V vs pseudo-RHE. The current density exhibited a
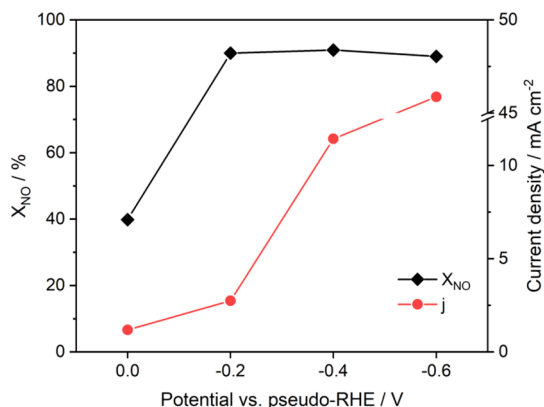

Figure 8. NO conversion (X_{NO}) and recorded current density as a function of applied potential (vs pseudo-RHE) during experiments with 983 ppm NO/He feed.

remarkably low value of ca. 1 mA cm^{-2}. The current density increased between -0.2 and -0.6 V and the NO conversion showed a relatively stable value of around 98%. The increase in current density is due to hydrogen evolution, as we detected increasing hydrogen concentrations with voltage in the outlet stream (Table S1).

The NORR performance reported in this work shows the great potential of this technology for NO_x abatement applications to pollutant abatement (N_2 formation) or value creation (NH_3 formation), greatly overcoming state-of-the-art technologies in terms of energy efficiency. The Ru catalyst was shown to selectively produce ammonia in NORR. However, if NORR to nitrogen is targeted, alternative catalysts such as Pd or Cu are worth investigating, as these were proven active in nitrate reduction to nitrogen.[26] These metals also have the advantage of being cheaper than Ru. The estimated energy consumption of the reported process, when the cell is operated with the oxygen evolution reaction at the anode, is ca. 8.8 kWh/kg NO_x. This is still higher than the energy consumption of SCR units, of approximately 0.89 kWh/kg NO_x. Nevertheless, with strategies to decrease cell voltage, such as the use of thinner electrolyte membranes and improved catalysts, it is possible to decrease the energy requirements of the electrochemical process.

■ CONCLUSIONS

The electrochemical conversion of NO to NH_3 in a PEM cell was investigated. A Ru/C catalyst afforded exceptional reaction performance with NO conversion reaching ca. 97% and FE of ca. 93% toward ammonia using a 4.8% NO/He feed. The recorded ammonia yield of 0.51 mmol cm^{-2} h^{-1} is among the highest reported to date. This is particularly promising for large-scale applications because all the advantages of PEM

cells, such as low Ohmic losses, good product separation, and relatively easy scalability, apply to NORR. Experiments with a 983 ppm NO feed, comparable to typical NO_x concentrations in car exhaust and power plant flue gas streams, were conducted and 98% conversion was achieved at potentials as low as 0 V, indicating that the PEM cell could be used as an alternative to state-of-the-art NO_x abatement technologies. The main advantages of such application are the *in situ* generation of reductant (hydrogen atom/molecule) and the low temperature (ca. 80 °C) at which the PEM cell operates, compared to 300 °C and above for SCR, three-way catalysis, and NO_x storage and reduction.

■ ASSOCIATED CONTENT

⑤ Supporting Information

The Supporting Information is available free of charge at https://pubs.acs.org/doi/10.1021/acscatal.3c01600.

> Experimental details, XRD characterization, TEM characterization, schematic of electrochemical NO reduction setup, X-ray diffractogram of the Ru/C catalyst, TEM micrograph, ammonia yield as a function of cell voltage for MEAs, faradaic efficiency toward hydrogen, H_2 concentration in the outlet stream, and current density as a function of flow rate (PDF)

■ AUTHOR INFORMATION

Corresponding Author

Atsushi Urakawa — *Catalysis Engineering, Department of Chemical Engineering, Delft University of Technology, 2629HZ Delft, The Netherlands;* ⑩ orcid.org/0000-0001-7778-4008; Email: A.Urakawa@tudelft.nl

Authors

Sorin Bunea — *Catalysis Engineering, Department of Chemical Engineering, Delft University of Technology, 2629HZ Delft, The Netherlands*

Manoj Coppens — *Catalysis Engineering, Department of Chemical Engineering, Delft University of Technology, 2629HZ Delft, The Netherlands*

Complete contact information is available at:
https://pubs.acs.org/10.1021/acscatal.3c01600

Author Contributions

The manuscript was written through contributions of all authors. All authors have given approval to the final version of the manuscript.

Notes

The authors declare no competing financial interest.

■ REFERENCES

(1) Kampa, M.; Castanas, E. Human health effects of air pollution. *Environ. Pollut.* **2008**, *151*, 362−367.

(2) Skalska, K.; Miller, J. S.; Ledakowicz, S. Trends in NO_x abatement: A review. *Sci. Total Environ.* **2010**, *408*, 3976−3989.

(3) Boerner, L. K. Industrial ammonia production emits more CO_2 than any other chemical-making reaction. Chemists want to change that. *Chemical and Engineering News*, **2019**; Vol. 97, Issue 24.

(4) Tian, H.; Liu, K.; Hao, J.; Wang, Y.; Gao, J.; Qiu, P.; Zhu, C. Nitrogen Oxides Emissions from Thermal Power Plants in China: Current Status and Future Predictions. *Environ. Sci. Technol.* **2013**, *47*, 11350−11357.

(5) Zhang, X.; Davidson, E. A.; Mauzerall, D. L.; Searchinger, T. D.; Dumas, P.; Shen, Y. Managing nitrogen for sustainable development. *Nature* **2015**, *528*, 51−59.

(6) Soloveichik, G. Electrochemical synthesis of ammonia as a potential alternative to the Haber−Bosch process. *Nat. Catal.* **2019**, *2*, 377−380.

(7) Suryanto, B. H. R.; Du, H.-L.; Wang, D.; Chen, J.; Simonov, A. N.; MacFarlane, D. R. Challenges and prospects in the catalysis of electroreduction of nitrogen to ammonia. *Nat. Catal.* **2019**, *2*, 290−296.

(8) Kyriakou, V.; Garagounis, I.; Vourros, A.; Vasileiou, E.; Stoukides, M. An Electrochemical Haber-Bosch Process. *Joule* **2020**, *4*, 142−158.

(9) Ampelli, C. Electrode design for ammonia synthesis. *Nat. Catal.* **2020**, *3*, 420−421.

(10) Eyde, H. S. The manufacture of nitrates from the atmosphere by the electric arc Birkeland-Eyde process. *J. R. Soc. Arts* **1909**, *57*, 568−576.

(11) Rouwenhorst, K. H. R.; Jardali, F.; Bogaerts, A.; Lefferts, L. From the Birkeland−Eyde process towards energy-efficient plasma-based NOX synthesis: a techno-economic analysis. *Energy Environ. Sci.* **2021**, *14*, 2520−2534.

(12) Wang, Y.; DeSilva, A. W.; Goldenbaum, G. C.; Dickerson, R. R. Nitric oxide production by simulated lightning: Dependence on current, energy, and pressure. *J. Geophys. Res.: Atmos.* **1998**, *103*, 19149−19159.

(13) Cherkasov, N.; Ibhadon, A. O.; Fitzpatrick, P. A review of the existing and alternative methods for greener nitrogen fixation. *Chem. Eng. Process.: Process Intesif.* **2015**, *90*, 24−33.

(14) Medford, A. J.; Hatzell, M. C. Photon-Driven Nitrogen Fixation: Current Progress, Thermodynamic Considerations, and Future Outlook. *ACS Catal.* **2017**, *7*, 2624−2643.

(15) Anand, M.; Abraham, C. S.; Nørskov, J. K. Electrochemical oxidation of molecular nitrogen to nitric acid − towards a molecular level understanding of the challenges. *Chem. Sci.* **2021**, *12*, 6442−6448.

(16) Hawtof, R.; Ghosh, S.; Guarr, E.; Xu, C.; Mohan Sankaran, R.; Renner Julie, N. Catalyst-free, highly selective synthesis of ammonia from nitrogen and water by a plasma electrolytic system. *Sci. Adv.* **2019**, *5*, No. eaat5778.

(17) Janssen, L. J. J.; Pieterse, M. M. J.; Barendrecht, E. Reduction of nitric oxide at a platinum cathode in an acidic solution. *Electrochim. Acta* **1977**, *22*, 27−30.

(18) Langer, S. H.; Pate, K. T. Electrogenerative reduction of nitric oxide. *Nature* **1980**, *284*, 434−435.

(19) Langer, S. H.; Pate, K. T. Selective electrogenerative reduction of nitric oxide. *Ind. Eng. Chem. Process Des. Dev.* **1983**, *22*, 264−271.

(20) Soto-Hernández, J.; Santiago-Ramirez, C. R.; Ramirez-Meneses, E.; Luna-Trujillo, M.; Wang, J.-A.; Lartundo-Rojas, L.; Manzo-Robledo, A. Electrochemical reduction of NOx species at the interface of nanostructured Pd and PdCu catalysts in alkaline conditions. *Appl. Catal., B* **2019**, *259*, No. 118048.

(21) Long, J.; Chen, S.; Zhang, Y.; Guo, C.; Fu, X.; Deng, D.; Xiao, J. Direct Electrochemical Ammonia Synthesis from Nitric Oxide. *Angew. Chem., Int. Ed.* **2020**, *59*, 9711−9718.

(22) Choi, J.; Du, H.-L.; Nguyen, C. K.; Suryanto, B. H. R.; Simonov, A. N.; MacFarlane, D. R. Electroreduction of Nitrates, Nitrites, and Gaseous Nitrogen Oxides: A Potential Source of Ammonia in Dinitrogen Reduction Studies. *ACS Energy Lett.* **2020**, *5*, 2095−2097.

(23) Kim, D.; Shin, D.; Heo, J.; Lim, H.; Lim, J.-A.; Jeong, H. M.; Kim, B.-S.; Heo, I.; Oh, I.; Lee, B.; Sharma, M.; Lim, H.; Kim, H.; Kwon, Y. Unveiling Electrode−Electrolyte Design-Based NO Reduction for NH$_3$ Synthesis. *ACS Energy Lett.* **2020**, *5*, 3647−3656.

(24) Ko, B. H.; Hasa, B.; Shin, H.; Jeng, E.; Overa, S.; Chen, W.; Jiao, F. The impact of nitrogen oxides on electrochemical carbon dioxide reduction. *Nat. Commun.* **2020**, *11*, 5856.

(25) Bunea, S.; Clemens, K.; Urakawa, A. Electrified conversion of contaminated water to value: selective conversion of aqueous nitrate to ammonia in a PEM cell. *ChemSusChem* **2022**, *15*, No. e202102180.

(26) Ampurdanés, J.; Bunea, S.; Urakawa, A. PEM Electrolysis-Assisted Catalysis Combined with Photocatalytic Oxidation towards Complete Abatement of Nitrogen-Containing Contaminants in Water. *ChemSusChem* **2021**, *14*, 1534−1544.

(27) Wan, H.; Bagger, A.; Rossmeisl, J. Electrochemical Nitric Oxide Reduction on Metal Surfaces. *Angew. Chem., Int. Ed.* **2021**, *60*, 21966−21972.

(28) Ko, B. H.; Hasa, B.; Shin, H.; Zhao, Y.; Jiao, F. Electrochemical Reduction of Gaseous Nitrogen Oxides on Transition Metals at Ambient Conditions. *J. Am. Chem. Soc.* **2022**, *144*, 1258−1266.

(29) Rosca, V.; Duca, M.; de Groot, M. T.; Koper, M. T. M. Nitrogen Cycle Electrocatalysis. *Chem. Rev.* **2009**, *109*, 2209−2244.

(30) Machida, M.; Sato, K.; Ishibashi, I.; Hasnat, M. A.; Ikeue, K. Electrocatalytic nitrate hydrogenation over an H+-conducting solid polymer electrolyte membrane−modified cathode assembly. *Chem. Commun.* **2006**, *7*, 732−734.

(31) Carmo, M.; Fritz, D. L.; Mergel, J.; Stolten, D. A comprehensive review on PEM water electrolysis. *Int. J. Hydrogen Energy* **2013**, *38*, 4901−4934.

(32) Cheng, X.; Zhang, J.; Tang, Y.; Song, C.; Shen, J.; Song, D.; Zhang, J. Hydrogen crossover in high-temperature PEM fuel cells. *J. Power Sources* **2007**, *167*, 25−31.

(33) Li, H.; Tang, Y.; Wang, Z.; Shi, Z.; Wu, S.; Song, D.; Zhang, J.; Fatih, K.; Zhang, J.; Wang, H.; Liu, Z.; Abouatallah, R.; Mazza, A. A review of water flooding issues in the proton exchange membrane fuel cell. *J. Power Sources* **2008**, *178*, 103−117.

(34) Gholami, F.; Tomas, M.; Gholami, Z.; Vakili, M. Technologies for the nitrogen oxides reduction from flue gas: A review. *Sci. Total Environ.* **2020**, *714*, No. 136712.